World Research Journal of Peptide and Protein
ISSN: 2278-4586 & E-ISSN: 2278-4608 Volume 2, Issue 1, 2013, pp.-052-058.
Available online at http://www.bioinfopublication.org/jouarchive.php?opt=&jouid=BPJ0000137

In Silico ANALYSIS OF PROTEIN - PROTEIN INTERACTION BETWEEN RESISTANCE AND VIRULENCE PROTEIN DURING LEAF RUST DISEASE IN WHEAT (*Triticum aestivum* L.)

KUMAR A.[1], MISHRA D.C.[1], RAI A.[1], SHARMA M.K.[2] AND GAJULA M.N.V.P.[1]*

[1]Centre for Agricultural Bioinformatics, IASRI, Library Avenue, New Delhi- 110 012, India.
[2]Department of Bioinformatics, J.V. College, Baraut- 250 611, UP, India.
*Corresponding Author: Email- mnvprasadgajula@gmail.com

Received: November 14, 2013; Accepted: December 05, 2013

Abstract- Wheat is a staple cereal crop and major food resource for majority population all over the world and it suffers from leaf rust disease which causes substantial loss in yield as well as grain quality. The leaf rust is a fungus disease caused by fungus *P. recondita f.sp. tritici*. Lr1, Lr10, Lr19, Lr34, Lr47 and Lr51 are resistance genes among many others while MAPK1 is a fungus protein causing leaf rust in wheat. Chemical control of rusts is expensive and hazardous to the environment. In present *In silico* study we generated the structure of MAPK1 and leaf rust resistance protein Lr1, Lr10, Lr19, Lr34, Lr47 and Lr51 using homology modeling. Reliability of the homology model was assessed by predicting MAPK1 secondary structure along with validation. The MAPK1 3D model was further evaluated by energy minimization algorithm. Protein-protein interaction between MAPK1 and leaf rust resistance proteins was studied by using a geometrical based docking program Patch Dock. Based on the result of protein-protein docking score and total atomic contact energy (ACE), interaction of MAPK1 was reported to be high with Lr51 and lowermost with Lr10. Furthermore force field studies also supported this phenomenon. The minimum docking score of Lr10 to MAPK1 indicate that it does not directly interact with pathogen protein during rust infection. It could be suggested that Lr51 is more interactive with MAPK1 then other leaf rust resistance genes which are found in wheat against rust disease. The results presented here could be useful in designing alternative resistance genes against wheat leaf rust disease.

Keywords- *Puccinia triticina*. MAPK1. Homology modeling, Protein-protein docking

Introduction

Wheat pertains to the Triticum genus of tribe Triticeae of the family Poaceae. It comprises diploid, tetraploid, and hexaploid species; (2n=2x=14), (2n=4x=28), (2n=6x=42) respectively. The hexaploid wheat, which is often described as 'bread wheat' that grows over a varied climatic and soil environments. Bread wheat comprises of three genomes A, B and D. *T. urartu* (2n=2x=14, AA) is considered as A genome donor to both tetra and hexaploid wheat [1,2] while *Aegiolops tauschii*, (syns.*Triticum tauschii*, *Aegiolops squarrosa*) is considered as D genome donor of hexaploid wheat [3]. There is still no unanimity on the progenitor of the B genome donor of both tetraploid and hexaploid wheat. Among crop plants wheat has the largest haploid genome size and recently it was approximately reported to be 17 Giga Base pair [4]. They identified between 94000 and 96000 genes, and assigned two thirds to the three component genomes (A, B and D). Rust disease is caused by *P. recondita* f.sp. *tritici* (Rob. ex. Desm. f.sp. atritici Eriks. & Henn.). *P. recondita* f. sp. tritici is the most dreadful pathogen which is adapted to a wide range of agro-climate and occurs in diverse wheat growing areas of the world [5,6]. More than seventy genes for leaf rust resistance (Lr), most of them major, seedling or race specific genes, have been catalogued to date in wheat [5,7,8]. Although the loss due to leaf rust is less damaging as compared to that of stripe rust and stem rust, still it causes greater annual loss due to its more frequent and widespread occurrence [9]. Yield losses due to cereal rust in the United States of America (USA) from 1918 to 1976, noting yield reduction of 50 % or more in epidemic year due to leaf rust [10,11]. In this study we examined the protein-protein interaction between resistance and pathogen/virulence protein MAPK1 at structural level using different bioinformatics algorithms including homology modeling, structure analysis & verification, energy minimizations, protein-protein docking, visualization tools (CHIMERA, PyMOL, and SPDBV) to annotate a bioinformatics approach for plant-pathogen interactions in plants.

Leaf rust resistance genes (viz., Lr1, Lr10, Lr19, Lr34, Lr47, Lr51) have been reported in *Triticun aestivum*.L [12-16]. MAPK1 (Mitogen Activated protein Kinase1) is a virulence protein showing pathogencity in *Puccinia triticina* [17]. MAPK1 is a member of gene family serine/threonine protein kinases known as mitogen-activated protein (MAP) kinases (MAPKs) [18]. MAPK1 are involved in the transduction of a variety of extracellular signals and the regulation of different developmental processes during Leaf rust infection in wheat [19,20].

In recent years, the study of interaction between resistance and virulence genes has been greatly promoted by the availability of their genomic sequences and resources for functional genomics analysis, including transcriptomics, proteomics and metabolomics. Although there is a report on the use of *in silico* approaches to identify the alternate resistant gene against yellow rust in wheat followed by protein interaction studies, there are no reports on such studies for leaf rust resistance in wheat.

MAP kinase homologous to the yeast Fus3/Kss1 MAP kinases have been identified in several fungal pathogens and found to be important for appressorium formation, invasive hyphal growth, and fungal pathogenesis [19]. In the budding yeast *Saccharomyces*

cerevisiae, five MAPK pathways are known to regulate mating, invasive growth, cell wall integrity, hyperosmoregulation, and ascospore formation [20]. Phylogenetic analysis indicated that PsMAPK1 is a YERK1 MAP kinase belonging to the Fus3/Kss1 class [21]. MAPK-docking sites of MEK1, MEK2, Ste7, Elk-1 and MAPK phosphatase (*MKP)-2* potently inhibit MEK2 phosphorylation of ERK2, ERK2 phosphorylation of Elk-1, and MKP-1 dephosphorylation of ERK2 [22] Ssk2/Ssk22-specific docking site in the Pbs2 N-terminal region of pbss MAPKK [23]. Docking interactions play an important role to determine connectivity of the yeast MAPKs Fus3 and Kss1. Homology models of four yeast MAPKs, FUS3, KSS1, HOG1 and MPK1 were built based on the X-ray structures of active and inactive rat ERK2 [24]. Thus, by keeping in view the above reasons, we studied the interaction of different leaf rust resistance genes with MAPK1 in order to understand the resistance mechanism at the structural level.

Materials and Methods

Sequence Analysis

The amino acid sequences of wheat leaf rust resistance protein Lr1 (Accession No-ABS29034), Lr10 (Accession No- AAQ01784), Lr19 (Accession No-ADL57138), Lr34 (Accession No-ADK62371), Lr47 (Accession No-CAB61891), and Lr51 (Accession No-AAT95396) were retrieved from the sequence database of NCBI (http://www.ncbi.nlm.nih.gov), and MAPK1 was extracted from the protein database Uniprot (http://www.uniprot.org) (accession no. A1BLL8 (A1BLL8_9BASI), 405aa).To identifies the templates for homology modeling of MAPK1, a BLASTP [25] search was performed against the RCSB Protein Data Bank [26] with the default parameters. (http://blast.ncbi.nlm.nih.gov/Blast.cgi)

Secondary Structure Prediction

Secondary structure prediction gives idea about structural pattern from the protein sequence in terms of helix, sheets and coils. Psipred program [27] was used to predict the structure of MAPK1 protein. The information obtained from the secondary structure of protein was considered to improve the sequence alignment between the target and template protein. Ramachandran plot z-score evaluation of MAPK1 protein was carried out by using What if server [28].

Homology Modeling

The three dimensional model of MAPK1 and leaf rust resistance proteins was predicted by using Swiss-Model [29-31] tool. Crystal structure of Fus3 PDB ID: 2B9F was used as template [32] for generated 3D structure of MAPK1. Swiss-Model is the fully dedicated server to automate modeling over the web. Model building was carried out with different steps of completive modeling. The model was selected on the base of sequence identity between template and target protein. The residue profiles and stereo-chemical properties of the predicted three-dimensional models of MAPK1 was further checked using ProSA-web, QMEAN, Rampage and PROCHECK servers [33-36].

Energy Minimization

Energy minimization was performed for the three dimensional model of MAPK1 by Chiron Rapid Energy Minimization server [37] (http://troll.med.unc.edu/chiron/documentation.php). This server reduces clash ratio of the model. Chiron minimizes the number of nonphysical atomic interactions (clashes) in the given protein structure.

Docking

Docking was performed with the help of the PatchDock [38]. It is geometry based molecular docking algorithm. The PatchDock algorithm divides the Connolly dot surface representation [39,40] of the molecules into concave, convex and flat patches. Then, complementary patches are matched in order to generate candidate transformations. Each candidate transformation is further evaluated by a scoring function that considers both geometric fit and atomic desolvation energy [41]. Finally, RMSD (root mean square deviation) clustering was applied to the candidate solutions to discard redundant solutions. The input parameters for the docking were the PDB coordinate file for the protein and the ligand molecule. This algorithm has three major stages (i) Molecular Shape Representation (ii) Surface Patch matching and (iii) Filtering and Scoring. The services are available at http://bioinfo3d.cs.tau.ac.il/ PatchDock/

Results

Sequence Analysis

The sequences of MAPK1 protein of *P.triticina* (accession no. A1BLL8 (A1BLL8_9BASI), 405aa) with unknown structure was taken from the UniProt (http://www.uniprot.org) protein sequence database. Sequences of wheat leaf rust resistance protein Lr1 (Accession No-ABS29034), Lr10 (Accession No- AAQ01784), Lr19 (Accession No-ADL57138), Lr34 (Accession No-ADK62371), Lr47 (Accession No-CAB61891), and Lr51 (Accession No-AAT95396) were retrieved from the sequence database of NCBI (http://www.ncbi.nlm.nih.gov) protein sequence database. Template MAPK protein of Fus3 was identified by using BLASTp showed 56% max identity with the target MAPK1. Pairwise sequence alignment of template and target using CLUSTALW [42] showed the conserved region in [Fig-1].

Fig. 1- Pairwise sequence alignment between model of MAPK1 and PDB entry 2B9F chain A through using CLUSTALW

Secondary Structure Prediction

PsiPred online server [27] identified the secondary structure of MAPK1 protein with distinct region of helices and stands [Fig-2]. The Ramachandran plot for the MAPK1 protein determines the phi-psi bond angle evaluation [Fig-3]. The Ramachandran plot showed about 92.8% residues in the favoured region, 4.6% residues in the

allowed region and 2.6% residues in the outlier region. Thus, overall 97.4% residues were found to be in allowed region. The QMEAN [36] score for the MAPK1 protein obtained as 0.686 showing acceptable range as per experimental value.

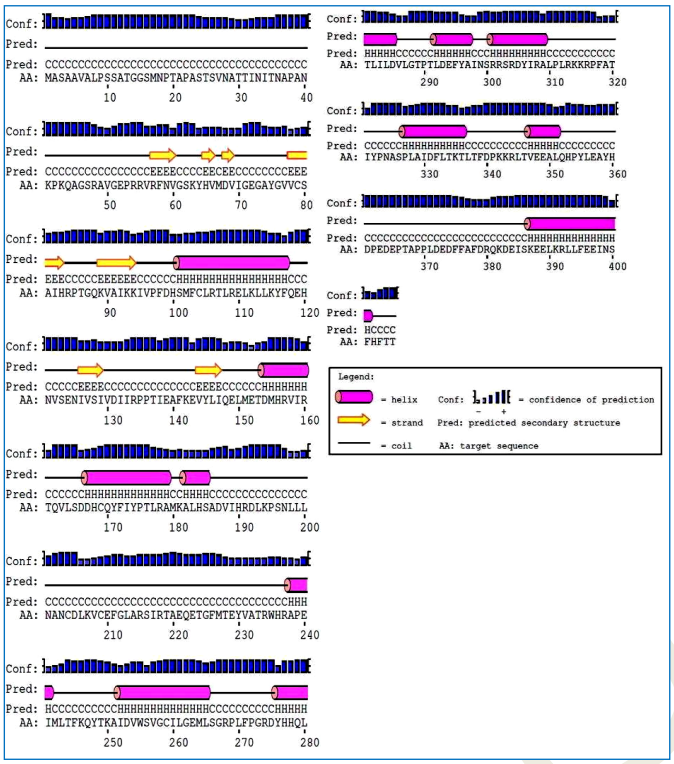

Fig. 2- PsiPred predicted secondary structure of MAPK1 protein

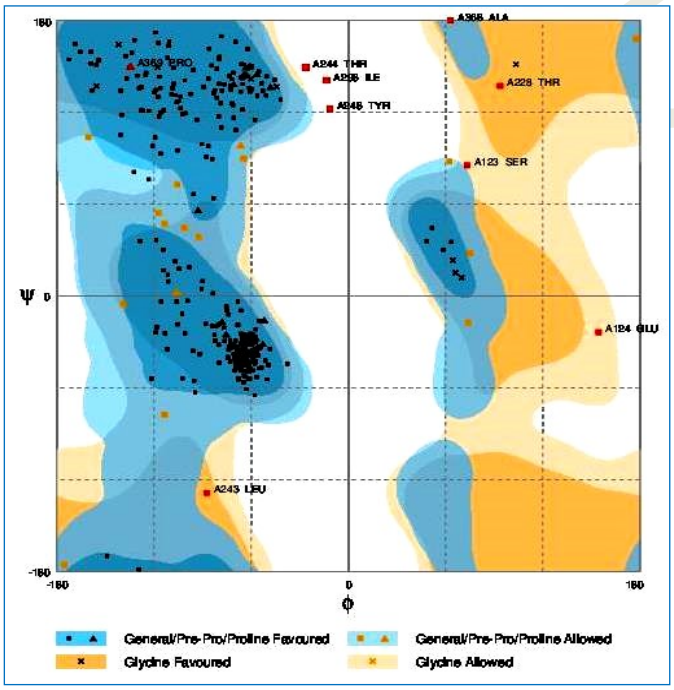

Fig. 3- Ramachandran plot for MAPK1 protein calculated by rampage

As the 3D structure of MAPK1 (405aa) of *Puccinia triticina* is not available in the protein data bank, we used homologous modeling in order to generate a 3D model of the MAPK1 protein [Fig-4]. A BLASTp search against PDB sequences was performed and result with maximum identity (3e-147 to 7e-136) was considered. The result identified 2b9f(353aa) in fus3, 2F9GA (Fus3 phosphorylated on tyr182, 353aa), 2B94A (Fus3 with docking motif, 353aa), 4IZ7C (Erk2 complexed with MAPK peptide, 356aa), 2Y9Q(Human Erk2 complexed with MAPK peptide, 362aa), 1WZYA(Erk2 in complex with fr148083, 368aa), 1TVOA(Erk2 with a small molecule inhibitor, 368aa) as potential templates for building 3D structure of MAPK1 (405aa). The sequence identity and similarity between target and templates was found to be 56% and 74% respectively [Fig-1]. The main chain parameters of the MAPK1 protein showed by the PROCHEK [26] [Fig-5]. The Goodness factor (G-factor, obtained from PROCHEK) is essentially a log-odds score based on the observed distribution of stereochemical parameters like quality of covalent and overall bond/angle distances. The G-factor obtained for modeled MAPK was 0.18 for dihedral,-0.11 for phi-psi, and 0.31 for overall. ProSA-web result reflects the good model quality on the knowledge based energy [Fig-6].

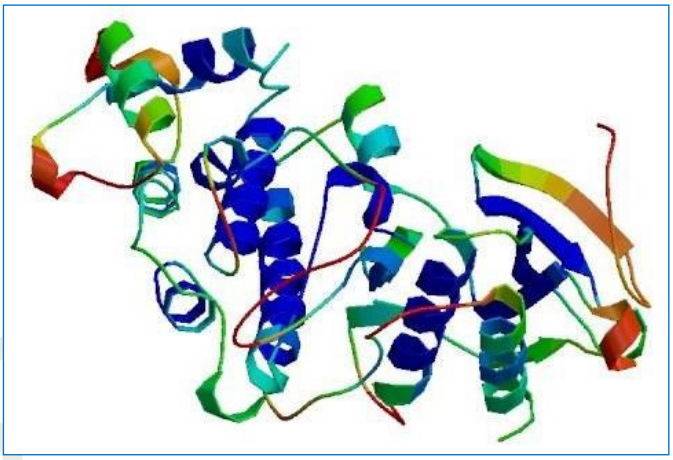

Fig. 4- Homology model of MAPK1 generated by Swiss-Model Homology Modeling

Swiss-Model (http://swissmodel.expasy.org/workspace) also were generated the 3D- Model of different resistance protein including Lr1, Lr10, Lr19, Lr34, and Lr51 on the base of comparative modeling Lr1 protein model were the 37.143% identity with template 1xkuA. Lr10 were the 31% identity with the template 3g06A, Lr19 were the 32% identity with 2p65A pdb template. Lr34 were the 34.375 identity with pdb template 3qf7A.and Lr51 were the 48.819 identity with pdb template 1yp3C [Table-1]. Phyre2 were generated the model of leaf resistance protein Lr47 on the base of sequence alignment to target protein c3s29C_template with 76% identity to chain C of sucrose synthase-1 protein of *Arabidopsis thaliana.*

Energy Minimization

Energy minimization was performed by Chiron Rapid Energy Minimization Server [37]. This server reduces clash ratio of the model. For MAPK1 model initially total numbers of clashes were 306,Total VDW repulsion energy was 244.954Kcal/mol and clash ratio was 0.0402355.The final numbers of clashes after energy minimization were 145,total VDW repulsion energy was 97.5808Kcal/mol and clash ratio was 0.0175221 [Table-2]. To compare the clash-score of the input and minimized structures to the benchmark set of 4300 high-resolution present in Chiron energy server, we plot the distribution of the normalized clash-score of the benchmark set and indicate the initial and final clash-score in the plot with respect to the distribution [Fig-7].

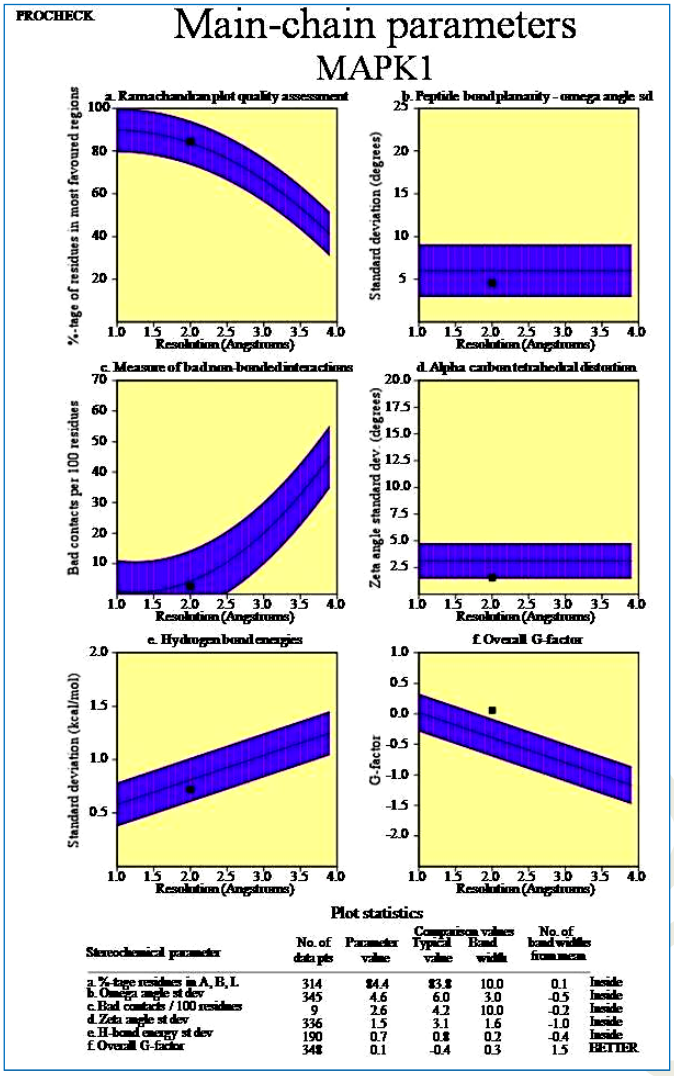

Fig. 5- Main-chain parameters for MAPK1 protein

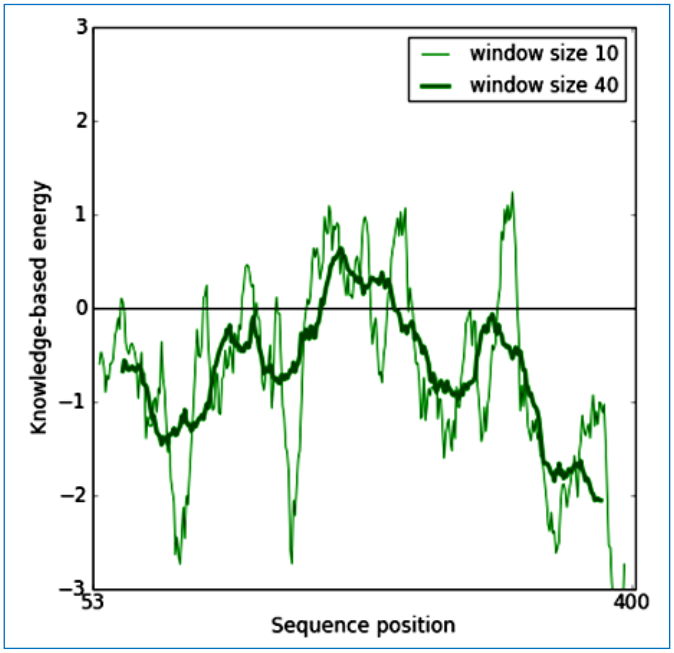

Fig. 6- ProSA-web predicted the knowledge base-energy graph for MAPK1 protein model

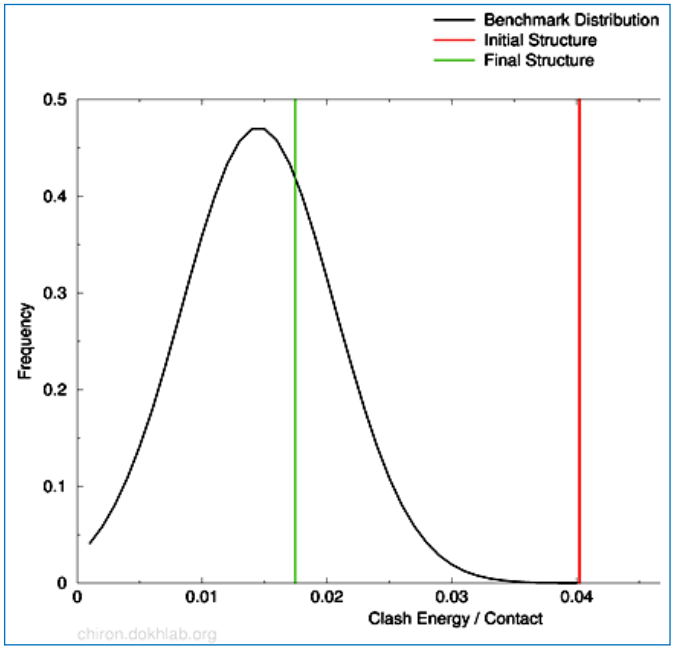

Fig. 7- Energy minimization graph of MAPK1 model Generated by chiron

Table 1- Homology modeling of wheat leaf rust resistance proteins

Protein	Template	Length (aa)	Sequence Identity (%)	Tool
Lr1	1xkuA	1344	37.143	Swiss-Model Workspace
Lr10	3g06A	921	30.952	Swiss-Model Workspace
Lr19	2p65A	878	31.915	Swiss-Model Workspace
Lr34	3qf7A	1402	34.375	Swiss-Model Workspace
Lr47	3s29C	60	76	Phyre2
Lr51	1yp3C	127	48.819	Swiss-Model Workspace

Table 2- Energy minimization of MAPK1 3D model by Chiron server

	No. of residues	No. of clashes	Clash ratio	Total VDW repulsion energy
Initial result (before energy minimization)	348	308	0.0402355	244.954 Kcal/mol
Final result (after energy minimization)	348	145	0.0175221	97.5808 Kcal/mol

Docking

Proteins are the basis of the life process at the molecular level. The protein interaction is either with other protein or with small molecules. Many biological studies, both in academia and in industry, may benefit from credible high- accuracy interaction predictions. Here we used PatchDock an algorithm for unbound (real life) docking of molecules, whether protein-protein or protein-drug. Goal of PatchDock docking algorithms is to detect a transformation of one of the molecules which brings it to optimal fit with the other molecule without causing steric clash depends not only on geometric, but also on biological criteria representing the resulting complex stability [43] PatchDock were generated the six solutions in Pdb format as a results of docking complexes of leaf rust resistance proteins and MAPK1 three dimensional models. Geometrical algorithm was give the ranked to a individual solution on the base of total applied transformation, covered area, score, ACE (atomic contact energy) and RMSD (4.0 by default) results shown in [Table-3]. Docking result reflected that MAPK1 maximum interactive with Lr51 and minimum interactive with Lr10. The docked complexes were analyzed with the molecular visualization tools, PyMOL as shown in

[Fig-8] GROMOS96 force-field algorithm were used over the Swiss PDB Viewer for calculate the total force- field Energy of docking solution, the total force field energy E=493325952.000 for bond, angles, improper, electrostatic of the docking solution.

Table 3- Protein-protein docking between MAPK1 and resistance proteins by PatchDock results

Receptor	Ligand	Score	Area	ACE	Transformation	Clustering RMSD
Lr1	MAPK1	12594	1700.2	-155.4	1.061.160.23 0.0743.61 -7.94	4.0
Lr10	MAPK1	11152	1623.2	-361.96	-1.26 -0.61 1.74 46.20 -31.0 27.07	4.0
Lr19	MAPK1	13000	1774.4	31.13	1.71 0.17 -0.45 -13.65 103.46 4.28	4.0
Lr34	MAPK1	11604	1383.7	10.13	-1.28 -1.06 -0.04 -67.36 -77.72 30.92	4.0
Lr47	MAPK1	14742	2591.3	133.6	0.73 -1.47 1.37 -81.76 -127.34 103.39	4.0
Lr51	MAPK1	15628	2263.6	250.3	-2.91 0.32 -2.76 56.24 -6.68 82.10	4.0

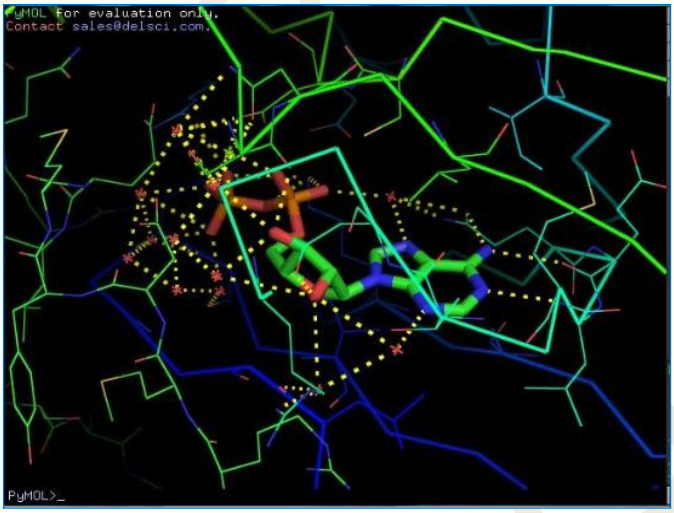

Fig. 8- Represantation of docking interaction between Lr51 and MAPK1 visualized by PyMOL

Discussions

The sequence analysis of the MAPK1 protein reveals that the MAPK1 protein sequence from the *P. triticina* was homologous with the MAPK protein sequence from the Fus3 with significant conserved region in it. This give green light we to use crystal structure of MAPK protein from Fus3 as a template for three dimensional structure predictions [46]. Secondary structure prediction is generally used to obtain some structural insight from the primary structure (amino acid sequences). The possible secondary structure for the MAPK1 protein also showed the number of helices, sheets and coils with desired level of confidence thus suggesting its stability [Fig-2]. The similarity between the template and target which was 56% for MAPK1 was found to be optimum for homology modeling. If the target and the template sequence share more than 50% sequence identity, prediction are of very good to high quality and have been shown to be as accurate as low-resolution X-ray predictions. [44,45]. Generated 3D modal was visualized by different macromolecule visualizations programs such as CHIMERA [46] and PyMoL [http://www.pymol.org/]. The predicted model comprise helices, beta sheets and loops. In Model evaluation results Ramachandran plot showed the number of residues in favored region are 92.8% and residues in allowed region 4.6% with overall allowed region [Fig-3] which reflect the predicted model is a good model. 3D model of MAPK1 have been successfully submitted in Protein model database (http://mi.caspur.it/PMDB/main.php) with ID PM0079053. The QMEAN score for the MAPK1 protein was found to be 0.686 that lies in the range of estimated model reliability value which is between 0 and 1 [36] suggesting the good quality of the model. After energy minimization final numbers of clashes were 145, total VDW repulsion energy was 97.5808Kcal/mol and clash ratio was 0.0175221.

Protein-protein docking is the only computational approach that directly models physical interactions between proteins [47,48]. However, it is necessary to cross compare the results obtained from in-silico computation with that of the experimental data like e.g, how it is done in several other studies [49,51]. High computational complexity restricts the flexible docking algorithms and is rarely applicable to practical protein docking at present. This problem can be overcome by using a rigid body docking algorithm [52]. The interaction MAPK1with resistance proteins were investigated with protein-protein docking. Docked results revealed that MAPK1 are more interacted with Lr51 than other gene during rust infection in wheat. Through this investigation we can suggest that Lr10 are more resistance against rust infection in wheat. We can perform wet-lab experiments using Immunoprecipitation (IP) technique to check the efficiency and accuracy of the presented *in silico* approach. It will accelerate the design of biological experiments to investigate interaction effect. This experiment could be useful for design an alternative resistance gene against wheat leaf rust disease.

Conclusions

In silico analysis of protein-protein interaction between six resistance and MAPK1 Protein was carried out at Structure level. After carried BLASTp for MAPK1 Protein structure it was found that it has 56% identities with the crystal structure of Non-Phosphorylated Fus3 on the basis of sequence alignment to PDB database. 3D structure Models of Leaf rust resistance proteins Lr1, Lr10, Lr19, Lr34, and Lr51 were generated by using the Swiss-Model algorithm. Lr47 3D Model was predicted by using Phyre2 based Algorithm. After using SAVES Statistical parameter for analysis & verification of crystal structure of Non-Phosphorylated Fus3 we have observed that it is useful for Protein-Protein Docking with different resistance Proteins 3D models. According to the best score 15628 of PatchDock result we have selected docking solution of Lr51 with MAPK1 protein Model for further analysis of docking solution. PyMOL has been used for showing the graphical interaction between receptor and ligand protein. SPDBV4.04 was predicted the Ramachandran plot of the docking solution and also calculate the total E=493325952.000 Force field energy of the docking solution.

Acknowledgement

MNV is acknowledging DST for the fellowship funding through SR/S2/RJN-22/2011.

Conflicts of Interest: None declared.

References

[1] Dvořák J., Terlizzi P.D., Zhang H.B. and Resta P. (1993) *Genome,* 36(1), 21-31.

[2] Dvorak J., McGuire P.E. and Cassidy B. (1988) *Genome*, 30(5), 680-689.

[3] Kihara H. (1944) *Agric. Hortic. Tokyo*, 19, 889-890.

[4] Brenchley R., Spannagl M., Pfeifer M., Barker G.L., D'Amore R., Allen A.M. and Hall N. (2012) *Nature*, 491(7426), 705-710.

[5] Kolmer J.A. (1996) *Annual Review of Phytopathology*, 34(1), 435-455.

[6] Kolmer J.A. and Ordoñez M.E. (2007) *Phytopathology*, 97(9), 1141-1149.

[7] Mclntosh R.A., Devos K.M., Dubcovsky J., Rogers W.J., Morris C.F., Appels R. and Anderson O.D. (2008) *Annual Wheat Newsletter*, 54, 209-225.

[8] Samsampour D., Zanjani B.M., Pallavi J.K., Singh A., Charpe A., Gupta S.K. and Prabhu K.V. (2010) *Euphytica*, 174(3), 337-342.

[9] Huerta-Espino J., Singh R.P., Germán S., McCallum B.D., Park R.F., Chen W.Q. and Goyeau H. (2011) *Euphytica,* 179(1), 143-160.

[10] Roelf A.P. (1978) *Misk. Publ. US Dept. Agric.,* 1363, 1-85.

[11] Sohail M., Khan M.A., Rashid A., Mateen A., Hussain M., Chohan M.A., Ahmad F., Latif M., Ahmad F. (2013) *Canadian Journal of Plant Protection*, 1(1), 15-27.

[12] Helguera M., Khan I.A. and Dubcovsky J. (2000) *TAG Theoretical and Applied Genetics,* 100, 1137-1143.

[13] Helguera M., Vanzetti I., Soria M., Khan I.A., Kolmer J. and Dubcovsky J. (2005) *Crop Science*, 45, 728-734.

[14] Krattinger S.G., Lagudah E.S., Wicker T., Risk J.M., Ashton A.R., Selter L.L. and Keller B. (2011) *The Plant Journal,* 65(3), 392-403.

[15] Ling H.Q., Zhu Y. and Keller B. (2003) *Theoretical and Applied Genetics,* 106(5), 875-882.

[16] Vanzetti L.S., Campos P., Demichelis M., Lombardo L.A., Aurelia P.R., Vaschetto L.M., Bainotti C.T., Helguera, M. (2011) *Electronic Journal of Biotechnology*, 14(3), 9-9.

[17] Hu G., Kamp A., Linning R., Naik S. and Bakkeren G. (2007) *Molecular Plant-microbe Interactions,* 20(6), 637-647.

[18] Zhang Y. and Dong C. (2007) *Cellular and Molecular Life Sciences,* 64(21), 2771-2789.

[19] Xu J.R. (2000) *Fungal Genetics and Biology,* 31(3), 137-152.

[20] Zhao X., Mehrabi R. and Xu J.R. (2007) *Eukaryotic Cell,* 6(10), 1701-1714.

[21] Guo J., Dai X., Xu J.R., Wang Y., Bai P., Liu F. and Kang Z. (2011) *PloS One,* 6(7), e21895.

[22] Bardwell L., Cook J.G., Chang E.C., Cairns B.R. and Thorner J.E.R.E.M.Y. (1996) *Molecular and Cellular Biology,* 16(7), 3637 -3650.

[23] Tatebayashi K., Takekawa M. and Saito H. (2003) *The EMBO Journal,* 22(14), 3624-3634.

[24] Smith D.L. and Nilar S.H. (2010) *Protein and Peptide Letters,* 17(6), 732-738.

[25] Altschul S.F., Gish W., Miller W., Myers E.W. and Lipman D.J. (1990) *Journal of Molecular Biology,* 215(3), 403-410.

[26] Bernstein F.C., Koetzle T.F., Williams G.J., Meyer E.F., Brice M.D., Rodgers J.R., Kennard O., Shimanouchi T. and Tasumi M. (1977) *J. Mol. Biol.,* 3, 532-542.

[27] Jones D.T. (1999) *J. Mol. Biol.,* 292, 195-200.

[28] Vriend G. (1990) *Journal of Molecular Graphics,* 8(1), 52-56.

[29] Arnold K., Bordoli L., Kopp J. and Schwede T. (2006) *Bioinformatics,* 22(2), 195-201.

[30] Kiefer F., Arnold K., Künzli M., Bordoli L. and Schwede T. (2009) *Nucleic Acids Research,* 37, 387-392.

[31] Peitsch M.C. (1995) *Bio/Technology,* 13, 658-660.

[32] Reményi A., Good, M.C., Bhattacharyya R.P. and Lim W.A. (2005) *Molecular Cell,* 20(6), 951-962.

[33] Wiederstein M. and Sippl M.J. (2007) *Nucleic Acids Res*., 35, 407-410.

[34] Laskowski R.A., MacArthur M.W., Moss D.S. and Thornton J.M. (1993) *Journal of Applied Crystallography,* 26(2), 283-291.

[35] Lovell S.C., Davis I.W., Arendall B.W., de Bakker P.I.W., Word J.M., Prisant M.G. and Richardson D.C. (2003) *Funct. Genet.,* 50, 437-450.

[36] Benkert P., Biasini M. and Schwede T. (2011) *Bioinformatics,* 27(3), 343-350.

[37] Ramachandran S., Kota P., Ding F. and Dokholyan N.V. (2011) *Proteins*, 79(1), 261-270.

[38] Schneidman-Duhovny D., Inbar Y., Polak V., Shatsky M., Halperin I., Benyamini H., Barzilai A., Dror O., Haspel N., Nussinov R., Wolfson H.J. (2003) *Proteins*, 52(1), 107-112.

[39] Connolly M.L. (1983) *Science,* 221(4612), 709-713.

[40] Connolly M.L. (1983) *J. Appl. Crystallogr.,* 16, 548-558.

[41] Zhang C., Vasmatzis G., Cornette J.L. and DeLisi C. (1997) *J. Mol. Biol.,* 267, 726.

[42] Thompson J.D., Gibson T.J., Plewniak F., Jeanmougin F. and Higgins D.G. (1997) *Nucleic Acids Research,* 25(24), 4876-4882.

[43] Dulvovny D., Nussian R., Wolfson H.J., Guigo R. and Gusfield D. (2002) *Springer, GmbH Rome,* 2452, 185-200.

[44] Kopp J. and Schwede T. (2004) *Pharmacogenomics,* 5(4), 405-416.

[45] Vitkup D., Melomud E., Moult J. and Sander C. (2001) *Nat .Struct. Biol.,* 8, 559-556.

[46] Pettersen E.F., Goddard T.D., Huang C.C., Couch G.S., Greenblatt D.M., Meng E.C. and Ferrin T.E. (2004) *Journal of Computational Chemistry,* 25(13), 1605-1612.

[47] Sternberg M.J., Gabb H.A. and Jackson R.M. (1998) *Current Opinion in Structural Biology,* 8(2), 250-256.

[48] Vajda S., Sippl M. and Novotny J. (1997) *Current Opinion in Structural Biology,* 7(2), 222-228.

[49] Gajula M.P., Vogel K.P., Rai A., Dietrich F. and Steinhoff H.J. (2013) *BMC Genomics,* 14(2), S4, 1-11.

[50] Gajula M.P. and Rai A. (2012) *Int. J. Systems Algorithms and Applications*, 2, 31-34.

[51] Gajula P., Borovykh I.V., Beier C., Shkuropatova T., Gast P.

and Steinhoff H.J. (2007) *Applied Magnetic Resonance*, 31(1-2), 167-178.

[52] Wenfan H. (2005) *Rigid body protein docking by Fast Fourier Transform*, Honours Year Project Report, School of Computing, National University of Singapore.

[53] Gupta S.K., Charpe A., Prabhu K.V. and Haque Q.M.R. (2006) *Theoretical and Applied Genetics,* 113(6), 1027-1036.

[54] Kolmer J.A. (2005) *Current Opinion in Plant Biology*, 8(4), 441-449.

[55] Oelke L.M. and Kolmer J.A. (2005) *Phytopathology,* 95(7), 773-778.

[56] Webster M.P., Jukes R., Zamfir V.S., Kay C.W., Bagnéris C. and Barrett T. (2012) *Nucleic Acids Research,* 40(17), 8743-8758.

[57] Gajula P., Milikisyants S., Steinhoff H.J., Huber M. (2007) *Applied Magnetic Resonance*, 31(1-2), 99-104.